Contribution from the Department of Chemistry,
Washington State University, Pullman, Washington 99164

Crystal Structure and Magnetic Properties of $[(C_2H_5)_2NH_2]_2(Cu_3Br_8)\cdot CuBr_2\cdot C_2H_5OH$: Magneto-Structural Correlations in Copper(II) Bromide Salts

R. FLETCHER, J. J. HANSEN, J. LIVERMORE, and R. D. WILLETT*

Received May 11, 1982

The crystal structure of the title compound, bis(diethylammonium) tetrabromotetrakis(μ-bromo)tricuprate(II)-copper(II) bromide-ethanol, has been determined. The monoclinic structure [a = 25.043 (8) Å, b = 6.4691 (14) Å, c = 19.009 (5) Å, and β = 102.84 (2)°; space group $C2/m$] contains two distinctly different copper(II) coordination environments. Planar, symmetrically bibridged $Cu_3Br_8^{2-}$ trimers (I) yield a square-planar geometry for three of the copper(II) ions. The Cu-Br

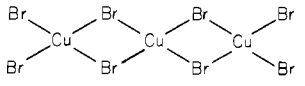

I

distances within the trimer average 2.421 Å, with a range from 2.365 to 2.500 Å. The Cu-Br-Cu bridging angles average 94.4°. The trimeric anions form stacks parallel to the b axis, with each copper completing its distorted-octahedral 4 + 2 coordination with bromide ions from adjacent trimers. The diethylammonium ions and ethanol molecule hydrogen bond to the anionic stack. In addition to the trimeric stack, an unusual neutral $CuBr_2$ chain also runs parallel to the b axis. In this symmetrically bibridged chain, each copper(II) ion has a distorted-tetrahedral coordination geometry, with Cu-Br distances of 2.394 and 2.427 Å. The two independent bridging Cu-Br-Cu angles are 84.2 and 84.3°. The magnetic susceptibility of the salt has been measured between 2.0 and 300 K. The results have been interpreted in terms of antiferromagnetic coupling within the trimers (J_t/k = -100 K) as well as within the chains (J_c/k = -20 K). The magneto-structural implications of these results for symmetrically bibridged systems are explored. In particular, it is shown that, as the coordination geometry is twisted from planar to tetrahedral, the exchange coupling is antiferromagnetic for planar and nearly tetrahedral coordination geometries and ferromagnetic for intermediate geometry.

Introduction

The structural and magnetic properties of copper halide salts continue to be of interest. Since Smith's comprehensive review of structural and electronic characteristics of copper chloride salts appeared in 1976,[1] several salts containing the previously unknown square-pyramidal coordination geometry have been reported: as an isolated $CuCl_5^{3-}$ ion in $(C_6H_{12}N_3H_3)CuCl_5\cdot 2H_2O$,[2] as part of the $Cu_3Cl_{14}^{8-}$ ion in $(C_6H_{12}N_3H_3)_4Cu_5Cl_{22}$,[3] and in the infinite bibridged chain structure in $(C_6H_{11}NH_3)CuCl_3$.[4] In several instances, it has also been demonstrated that two or more stereochemistries can exist in the same salt. The above mentioned $(C_6H_{12}N_3H_3)_4Cu_5Cl_{22}$ contains distorted-tetrahedral $CuCl_4^{2-}$ ions and a copper ion with 4 + 2 elongated-octahedral coordination as well as the square-pyramidal coordination.[3] Distorted-tetrahedral and 4 + 2 elongated-octahedral coordination also coexist in $[(CH_3)_3NH]_3Cu_2Cl_7$.[5] In the room-temperature phase of $[(CH_3)_2CHNH_3]_2CuCl_4$, both 4 + 1 and 4 + 2 coordination geometries exist, with the 4 + 1 geometry intermediate between a square pyramid and the discrete distorted-tetrahedral geometry of $CuCl_4^{2-}$ and Cl^- ions.[6] The room-temperature structure of $[(C_2H_5)_2NH_2]_2CuCl_4$ contains three independent $CuCl_4^{2-}$ ions with different degrees of tetrahedral distortion.[7] In addition, the phenomena of discontinuous thermochromism in both the chloride and bromide salts have demonstrated that it is possible to interconvert between different stereochemistries in the solid state.[8-10]

The correlation of magnetic properties with stereochemistry is a subject of interest in inorganic chemistry, with extensive work being done on hydroxy-bridged[11] and alkoxy-bridged[12] copper(II) dimers, oxygen-bridged chromium(III) dimers,[13] and mixed-metal systems,[14,15] to name a few examples. The elucidation of magneto-structural correlations in copper(II) chloride salts is one of the current activities in our laboratory.[8,10,16-18] This is rendered difficult not only by the diversity of geometries described above but also by the rather small range of values of the exchange constant, J, exhibited by the chloride salts. Typical values for antiferromagnetic interaction generally are $J/k \sim -10$ to -25 K. For the corresponding bromides, however, these values frequently range down to -100 K. Thus, the bromide salts are more attractive candidates for investigation of these magneto-structural correlations.

Unfortunately, the stereochemistry of copper(II) bromide salts is not nearly so thoroughly documented. It is usually assumed that the bromide salts are isomorphous with the corresponding chloride salts. This frequently is true,[8,10,16] but notable exceptions exist, e.g., $CsCuCl_3$[19] and $CsCuBr_3$.[20] Thus, it is imperative to have precise structural information

(1) D. W. Smith, *Coord. Chem. Rev.*, **21**, 93 (1976).
(2) L. Antolini, G. Marcotrigiano, L. Menabue, and G. C. Pellaconi, *J. Am. Chem. Soc.*, **102**, 1303 (1980).
(3) L. Antolini, G. Marcotrigiano, L. Menabue, and G. C. Pellaconi, *J. Am. Chem. Soc.*, **102**, 5506 (1980).
(4) H. A. Groenendijk, H. W. J. Blote, A. J. van Duyneveldt, R. M. Gaura, C. P. Landee, and R. D. Willett, *Physica B+C (Amsterdam)*, **106B+C**, 47 (1981).
(5) R. M. Clay, P. Murray-Rust, and J. Murray-Rust, *J. Chem. Soc., Dalton Trans.*, 595 (1973).
(6) D. N. Anderson and R. D. Willett, *Inorg. Chim. Acta*, **8**, 167 (1974).
(7) S. Simonsen, private communication.
(8) S. A. Roberts, D. R. Bloomquist, R. D. Willett, and H. W. Dodgen, *J. Am. Chem. Soc.*, **103**, 2603 (1981).
(9) D. R. Bloomquist, R. D. Willett, and H. W. Dodgen, *J. Am. Chem. Soc.*, **103**, 2610 (1981).
(10) D. R. Bloomquist and R. D. Willett, *J. Am. Chem. Soc.*, **103**, 2615 (1981).
(11) V. H. Crawford, H. W. Richardson, J. R. Wasson, D. J. Hodgson, and W. E. Hatfield, *Inorg. Chem.*, **15**, 2107 (1976).
(12) R. Mergehenn, L. Merz, and W. Haase, *J. Chem. Soc., Dalton Trans.*, 1703 (1980); L. Merz and W. Haase, *J. Chem. Soc., Dalton Trans.*, 875 (1980).
(13) R. P. Scaringe, D. J. Hodgson, and W. E. Hatfield, *Transition Met. Chem.*, **6**, 340 (1981).
(14) O. Kahn, R. Claude, and H. Coudanne, *J. Chem. Soc., Chem. Commun.*, 1012 (1978); Y. Journaux and O. Kahn, *J. Chem. Soc., Dalton Trans.*, 1575 (1979).
(15) L. Banci, A. Bencini, A. Dei, and D. Gatteschi, *Inorg. Chem.*, **20**, 393 (1981); L. Banci, A. Bencini, C. Benelli, A. Dei, and D. Gatteschi, *ibid.*, **20**, 1399 (1981).
(16) G. O'Bannon and R. D. Willett, *Inorg. Chim. Acta*, **53**, L131 (1981).
(17) J. C. Livermore, R. D. Willett, R. M. Gaura, and C. P. Landee, *Inorg. Chem.*, **21**, 1403 (1982).
(18) R. D. Willett and C. P. Landee, *J. Appl. Phys.*, **52**, 2004 (1981).
(19) A. W. Schlueter, R. A. Jacobson, and R. E. Rundle, *Inorg. Chem.*, **5**, 277 (1966).
(20) T. Li and G. D. Stucky, *Inorg. Chem.*, **12**, 441 (1973).

0020-1669/83/1322-0330$01.50/0

on more copper(II) bromide salts.

In the course of study of a series of thermochromic copper halides,[7-10] a diethylammonium salt with unusual stoichiometry was obtained. For the reasons indicated above, a structural and magnetic investigation was pursued, the results of which are reported herein.

Experimental Section

Preparation. The compound $(DEA)_2Cu_4Br_{10}\cdot EtOH$ [DEA = the diethylammonium ion, $(C_2H_5)_2NH_2^+$] was prepared by combining 90 g (0.58 mol) of (DEA)Br with 150 g of $CuBr_2$ (0.62 mol) in 400 mL of pure ethanol. The solution was stirred for 2 h, and the insoluble material was separated by filtration. After the filtrate stood at room temperature for 24 h, the temperature was increased to 60 °C and the solution was heated to dryness. The solid was redissolved in ethanol, filtered, and set aside at room temperature. Long deep-purple crystals were collected after 7 days and washed in ether. Anal. Calcd: C, 9.75; N, 2.27; H, 2.46. Found: C, 9.66; N, 2.30; H, 2.46.

X-ray Crystallography. Data were collected for $(DEA)_2Cu_4Br_{10}\cdot EtOH$ by using a single crystal with dimensions 0.009 cm × 0.013 cm × 0.024 cm (volume 2.5×10^{-3} mm^3). Systematic extinctions ($h + k = 2n + 1$ for hkl reflections) defined the space group as $C2$, Cm, or $C2/m$. The lattice constants, determined from a least-squares refinement on 12 well-centered reflections, are a = 25.043 (8) Å, b = 6.4691 (14) Å, c = 19.009 (5) Å, and $\cos\beta$ = −0.2223 (4). The calculated density is 2.760 g cm^{-3} (4 molecules/unit cell). A total of 1905 reflections were collected on an automated Picker four-circle diffractometer using Zr-filtered Mo Kα radiation (λ = 0.710 69 Å). A θ–2θ step scan was used with a 0.05° step size, a 2.0° peak width, and a 2 s/step count. Background was counted for 10 s before and after each scan. The intensities of three reflections were monitored every 40 reflections to check for decomposition. Linear decay and absorption corrections were applied (μ = 169.98 cm^{-1}; transmission factors ranging from 0.13 to 0.24). The standard deviation of each reflection was calculated by $\sigma^2(I)$ = TC + BG + 0.03^2I^2, where TC is total counts, BG is background counts, and I = TC − BG. Computer programs were part of a local program library.[21]

Magnetic data collection was made on a PAR vibrating-sample magnetometer, over a temperature range of 1.9–300 K. An applied magnetic field of 3349 G was used for the temperature range of 1.9–85 K, and a field of 7250 G was applied from 85 to 300 K. A germanium resistance thermometer was used for the low-temperature range, and a thermocouple was used to measure higher temperatures. The diamagnetic correction term was -520.9×10^{-6} emu/mol, and the temperature-independent paramagnetism was taken as 240×10^{-6} emu/mol.

Structure Solution. The intensity-weighted reciprocal lattice showed a strong subcell relationship associated with polymeric copper halide species as previously noted for $Cu_3Cl_6(CH_3CN)_2$,[22] $Cu_5Cl_{10}(C_3H_7OH)_2$,[22] and $[(CH_3)_3NH]_2Cu_4Cl_{10}$.[23] In addition, the repeat distance along the needle axis of approximately 6 Å led to the initial assumption of a herringbone structure of nearly planar $Cu_4Br_{10}^{2-}$ anions. This would require the use of the noncentric space group $C2$. At first glance, this seemed to be in accord with the Patterson function, since the Harker line at (u, v, w) = (0, $2y$, 0) (due to a mirror plane perpendicular to the b axis) showed no peaks except at v = 0 and $^1/_2$. However, closer examination of the total Patterson function revealed that it had peaks essentially only at v = 0 and $^1/_2$. This indicated that the mirror planes actually were present (e.g., space group $C2/m$), with most of the atoms located on the mirror planes at y = 0 and $^1/_2$. In addition, the Patterson section at $v = {}^1/_4$ contained a series of peaks, centered at (u, v, w) = ($^1/_2$, $^1/_4$, $^1/_4$), which could be decomposed into the overlapping images of two planar $Cu_3Br_8^{2-}$ anions. This was interpreted to mean the presence of a heavy atom (Cu^{2+} or Br^-) at 0, $^1/_4$, 0 (on a twofold axis at x = 0, z = 0), with the $Cu_3Br_8^{2-}$ anion lying on the mirror planes at y = 0 (and $y = {}^1/_2$) near the 2_1 axis at $x = {}^1/_2$, $z = {}^1/_4$. An electron-density map phased on this model showed the existence of two additional peaks on the mirror planes, near the twofold axis. From this, it was possible to identify a $(CuBr_2)_n$ chain running parallel to the b axis. Subsequent electron-density and difference electron-density maps allowed the identification of the DEA cations and the EtOH molecule. The nitrogen atoms of the DEA cations lie on the mirror plane and are hydrogen bonded to the $Cu_3Br_8^{2-}$ trimers. One arm of each cation also lies on the mirror plane. However, steric constraints appear to prohibit the other arm from doing so, and it was found to be disordered across the mirror plane. No attempt was made to vary the y parameters of the disordered carbon atoms, so that structural characteristics reported must be interpreted in that light. The EtOH molecule was found to be disordered about the twofold axis passing through $x = {}^1/_2$, $z = {}^1/_2$. Reasonable locations, based on the electron-density maps, were assigned to the atoms, but it proved to be impossible to refine the positions. The high R value for the final refinement ($R_1 = \sum||F_o| - |F_c||/|F_o| = 0.087$; $R_2 = \sum w(|F_o| - |F_c|)^2/\sum|F_o|^2 = 0.089$) is due to two factors. As noted previously,[24] copper(II) bromide salts are always subject to light and/or thermal decomposition, so that accurate structure refinements are seldom attained. Also, in this case, the observed disorder in the DEA cations implies that the $Cu_3Br_8^{2-}$ anions are disordered across the mirror planes. Thus, the thermal parameters are not able to properly compensate for the actual electron density. Large peaks on the difference maps were observed in the region of the heavy atoms, in accord with these two observations. Indeed, in the final refinement, the bromine atoms lying on the edge of the stack were displaced slightly off the mirror plane, and the restrictions on their thermal parameters relaxed, in order to better fit the electron density in that region of space. Final parameters are reported in Table I, and bond distances and angles are reported in Tables II and III, respectively.

Table I. Positional Parameters for $(DEA)_2Cu_4Br_{10}\cdot EtOH$

atom	x	y	z
Cu(1)	0.2960 (2)	0.0	0.2796 (3)
Cu(2)	0.2340 (2)	0.0	0.4330 (3)
Cu(3)	0.1671 (2)	0.0	0.5804 (3)
Br(1)	0.2552 (2)	0.02000	0.1543 (3)
Br(2)	0.2038 (2)	0.02000	0.3044 (3)
Br(3)	0.1417 (2)	0.02000	0.4484 (3)
Br(4)	0.0735 (2)	0.02000	0.5844 (3)
Br(5)	0.2004 (2)	0.0	0.7082 (2)
Br(6)	0.2630 (2)	0.0	0.5632 (2)
Br(7)	0.3262 (2)	0.0	0.4141 (2)
Br(8)	0.3884 (2)	0.0	0.2657 (3)
Cu(4)	0.0	0.2516 (8)	0.0
Br(9)	0.0655 (2)	0.0	0.0626 (4)
Br(10)	0.4726 (3)	0.0	0.0784 (3)
C(11)	−0.011 (3)	0.10000	0.738 (4)
C(12)	0.024 (5)	0.10000	0.758 (6)
N(1)	0.084 (2)	0.0	0.778 (2)
C(13)	0.090 (3)	0.0	0.855 (4)
C(14)	0.146 (3)	0.0	0.884 (3)
C(24)	0.388 (3)	0.10000	0.777 (4)
C(22)	0.340 (4)	0.03000	0.920 (5)
C(21)	0.308 (3)	0.03000	0.965 (4)
N(2)	0.315 (2)	0.0	0.850 (3)
C(23)	0.359 (3)	0.04688	0.808 (4)
C(3)	0.459 (3)	0.0	0.596 (5)
O(1)	0.479 (4)	0.0	0.484 (7)
C(2)	0.539 (4)	0.0	0.458 (7)

Structure Description. The structure contains many interesting features. The salt contains two independent copper bromide sublattices: a $(CuBr_2)_n$ chain and a stack of $Cu_3Br_8^{2-}$ trimers. Both have unusual features associated with them, which have not previously been observed in copper halide salts.

Attention will first be focused on the bibridged chain, which is illustrated in Figure 1. This is a neutral chain, with distorted-tetrahedral coordination geometry about the copper ion. Only in anhydrous $CuCl_2$[25] and $CuBr_2$[26] are neutral chains known, and these have planar coordination geometry, with the fifth and sixth octahedral sites occupied by halide ions from adjacent chains. As seen from the thermal ellipsoids of the bromide atoms, these chains are undergoing rather large torsional oscillations around the chain axis. This is not

(21) D. N. Anderson, Ph.D. Thesis, Washington State University, 1971; R. E. Caputo, Ph.D. Thesis, Washington State University, 1976.
(22) R. D. Willett and R. E. Rundle, *J. Chem. Phys.*, **40**, 838 (1964).
(23) R. E. Caputo, M. J. Vukosavovich, and R. D. Willett, *Acta Crystallogr., Sect. B.*, **B32**, 2516 (1976).
(24) D. D. Swank and R. D. Willett, *Inorg. Chem.*, **19**, 2321 (1980).
(25) A. F. Wells, *J. Chem. Soc.*, 1670 (1947).
(26) L. Helmholz, *J. Am. Chem. Soc.*, **69**, 886 (1947).

Table II. Interatomic Distances (Å) in $[(C_2H_5)_2NH_2]_2(Cu_3Br_{10})\cdot CuBr_2\cdot C_2H_5OH$

		Trimer	
Cu(1)-Br(1)	2.378 (8)	Cu(3)-Br(4)	2.365 (6)
Cu(1)-Br(8)	2.388 (6)	Cu(3)-Br(5)	2.388 (6)
Cu(1)-Br(2)	2.458 (6)	Cu(3)-Br(3)	2.451 (7)
Cu(1)-Br(7)	2.500 (6)	Cu(3)-Br(6)	2.496 (6)
Cu(2)-Br(3)	2.396 (6)	Cu(1)-Cu(2)	3.595 (6)
Cu(2)-Br(2)	2.397 (7)	Cu(2)-Cu(3)	3.569 (6)
Cu(2)-Br(7)	2.414 (6)		
Cu(2)-Br(6)	2.420 (6)		
		Intertrimer	
Cu(1)-Br(5)	3.243 (1)	Cu(3)-Br(7)	3.239 (1)
Cu(2)-Br(6)	3.236 (1)		
		Chain	
Cu(4)-Br(10)	2.394 (5)	Cu(4)-Cu(4)	3.214 (10)
Cu(4)-Br(9)	2.427 (5)	Cu(4)-Cu(4)′	3.255 (10)
		Diethylammonium	
C(11)-C(12)	1.55 (6)	C(21)-C(22)	1.34 (8)
C(12)-N(1)	1.61 (10)	C(22)-N(2)	1.35 (8)
N(1)-C(13)	1.44 (7)	N(2)-C(23)	1.54 (7)
C(13)-C(14)	1.38 (8)	C(23)-C(24)	1.40 (6)
		Ethanol	
O(1)-C(2)	1.68 (6)	C(2)-C(3)	1.04 (11)
		Hydrogen Bonding	
N(1)-Br(8)	3.45 (1)	N(2)-Br(5)	3.47 (5)
N(1)-Br(5)	3.46 (4)	N(2)-Br(1)	3.55 (2)
N(1)-Br(4)	3.63 (4)	N(2)-Br(1)′	3.79 (2)
O(1)-Br(4)	3.51 (4)		
O(1)-Br(4)	3.74 (4)		
O(1)-Br(7)	3.77 (10)		

Table III. Interatomic Angles (deg) in $[(C_2H_5)_2NH_2]_2(Cu_3Br_8)\cdot CuBr_2\cdot C_2H_5OH$

		Trimer	
Br(1)-Cu(1)-Br(8)	95.7 (2)	Br(4)-Cu(3)-Br(5)	95.2 (2)
Br(1)-Cu(1)-Br(2)	88.8 (2)	Br(4)-Cu(3)-Br(3)	90.0 (2)
Br(1)-Cu(1)-Br(7)	174.8 (2)	Br(4)-Cu(3)-Br(6)	176.8 (2)
Br(8)-Cu(1)-Br(2)	174.8 (2)	Br(5)-Cu(3)-Br(3)	176.9 (2)
Br(8)-Cu(1)-Br(7)	91.9 (2)	Br(5)-Cu(3)-Br(6)	90.2 (2)
Br(2)-Cu(1)-Br(7)	83.6 (2)	Br(3)-Cu(3)-Br(6)	84.5 (2)
Br(3)-Cu(2)-Br(2)	91.7 (2)	Cu(1)-Br(2)-Cu(2)	95.5 (2)
Br(3)-Cu(2)-Br(7)	179.7 (1)	Cu(2)-Br(3)-Cu(3)	94.8 (2)
Br(3)-Cu(2)-Br(6)	87.6 (2)	Cu(2)-Br(6)-Cu(3)	93.1 (2)
Br(2)-Cu(2)-Br(7)	86.7 (2)	Cu(1)-Br(7)-Cu(2)	94.0 (2)
Br(2)-Cu(2)-Br(6)	179.9 (1)		
Br(7)-Cu(2)-Br(6)	94.1 (2)		
		Intertrimer	
Br(5)-Cu(1)-Br(5)	171.9 (2)	Br(7)-Cu(3)-Br(7)	173.7 (2)
Br(6)-Cu(2)-Br(6)	176.8 (3)		
		Chain	
Br(10)-Cu(4)-Br(10)′	95.7 (2)	Cu(4)-Br(9)-Cu(4)	84.2 (2)
Br(10)-Cu(4)-Br(9)	113.6 (2)	Cu(4)-Br(10)-Cu(4)	84.3 (2)
Br(10)-Cu(4)-Br(9)′	120.0 (2)		
Br(9)-Cu(4)-Br(9)′	95.3 (2)		
		Diethylammonium Ions	
C(11)-C(12)-N(1)	100 (3)	C(21)-C(22)-N(2)	112 (8)
C(12)-N(1)-C(13)	97 (5)	C(22)-N(2)-C(23)	105 (6)
N(1)-C(13)-C(14)	106 (6)	N(2)-C(23)-C(24)	126 (2)
		Ethanol	
O(1)-C(2)-C(3)	122 (11)		
		Hydrogen Bonding	
C(12)-N(1)-Br(8)	123 (2)	C(13)-N(1)-Br(8)	105 (1)
C(12)-N(1)-Br(5)	137 (4)	C(13)-N(1)-Br(5)	119 (4)
C(12)-N(1)-Br(4)	84 (4)	C(13)-N(1)-Br(4)	178 (2)
C(22)-N(2)-Br(5)	152 (5)	C(23)-N(2)-Br(5)	99 (4)
C(22)-N(2)-Br(1)	98 (2)	C(23)-N(2)-Br(1)	114 (1)
C(22)-N(2)-Br(1)	98 (2)	C(23)-N(2)-Br(1)	112 (1)
C(2)-O(1)-Br(4)	100 (4)		
C(2)-O(1)-Br(4)	99 (4)		
C(2)-O(1)-Br(7)	143 (8)		

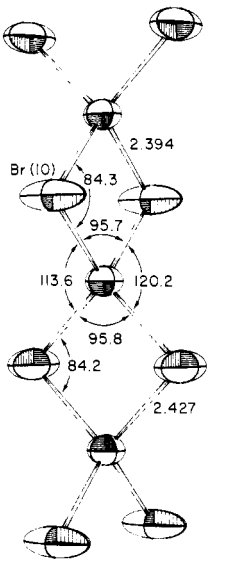

Figure 1. Neutral $CuBr_2$ chain in $[(C_2H_5)_2NH_2]_2(Cu_3Br_8)\cdot CuBr_2\cdot C_2H_5OH$.

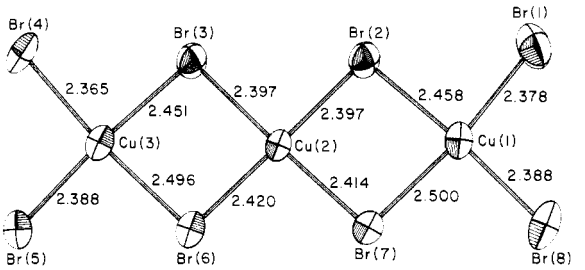

Figure 2. Illustration of the $Cu_3Br_8^{2-}$ trimer.

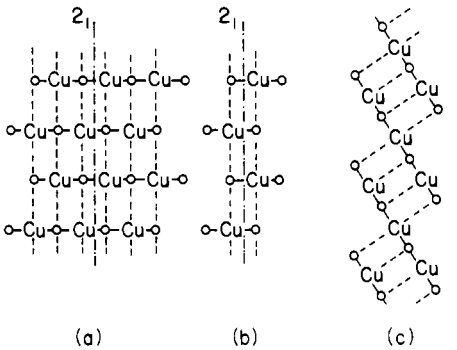

Figure 3. Schematic illustration of trimers: right-hand side, stacking as found in $Cu_3Cl_6(H_2O)_2\cdot 2TMSO_2$ and $Cu_3Cl_6(CH_3CN)_2$; left-hand side, stacking as found in $[(C_2H_5)_2NH_2]_2(Cu_3Br_8)\cdot CuBr_2\cdot C_2H_5OH$; center, end view of the same.

surprising, since there are no hydrogen-bonding interactions to anchor the chain in position. Thus, the chain is free to twist, constrained only by packing considerations. In view of the lack of hydrogen-bonding interactions, the distorted-tetrahedral coordination geometry is not surprising either. Experimentally, it has been shown that with fewer hydrogen bonds (or other electrostatic interactions) the copper halide chromophore tends to distort more toward tetrahedral geometry.[9] Note that the distortion of the copper coordination geometry is such that the pseudo-S_4 axis is perpendicular to the chain. The angle between the Br(9)-Cu(4)-Br(9) and Br(10)-Cu(4)-Br(10) planes is 84.9°.

The trimer species is not quite so unusual. The structures of the planar, bibridged trimeric species $Cu_3Cl_6(CH_3CN)_2$[17] and $Cu_3Cl_6(H_2O)_2$ (the latter in $Cu_3Cl_6(H_2O)_2\cdot 2TMSO_2$)[27] have been reported. This is, however, the first extended bibridged copper bromide polymer reported, as well as the first anionic trimer. The bond distances and

(27) D. D. Swank and R. D. Willett, *Inorg. Chim. Acta*, **8**, 143 (1974).

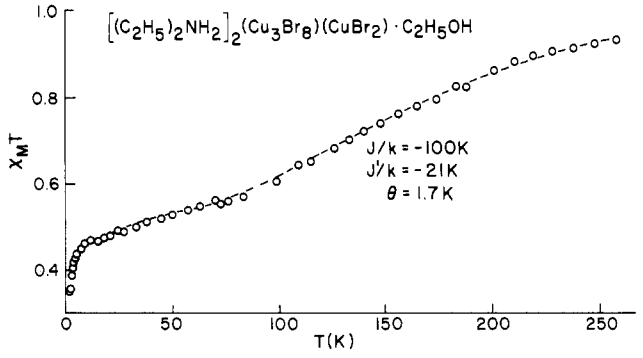

Figure 4. Plot of $\chi_M T$ vs. T for $[(C_2H_5)_2NH_2]_2(Cu_3Br_8)\cdot CuBr_2\cdot C_2H_5OH$.

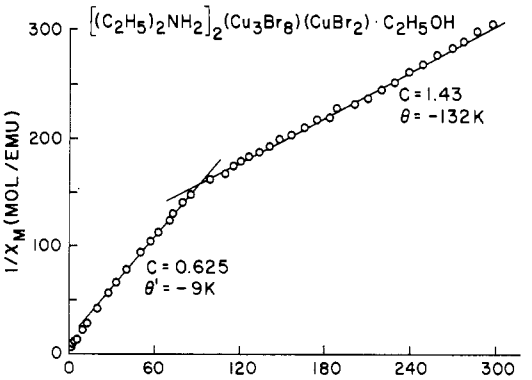

Figure 5. Plot of $1/\chi_M$ vs. T for $[(C_2H_5)_2NH_2]_2(Cu_3Br_8)\cdot CuBr_2\cdot C_2H_5OH$.

angles within the trimer are all normal (see Tables II and III and Figure 2). What is unique about the trimers, however, is the manner in which they stack. In all other extended polymers, the normal to the polymer makes a large angle with the stacking axis, as depicted in Figure 3c, and the polymers stack in a herringbone fashion. However, in this compound, the normal to the trimer is parallel to the stacking axis, as shown in Figure 3a,b. The trimers are situated with respect to the 2_1 screw axis such that each copper atom completes its 4 + 2 coordination geometry with a bromide atom from the trimer directly above and below it. As seen in Figure 3b, the stacking is such that one edge of the trimer sticks out from the stack (Br(1) through Br(4)) while the other edge is clamped between adjacent trimers. The trimer behaves similarly to a springboard: The thermal amplitudes of vibration of the bromine atoms on the clamped edge are small, but those of Br(1) through Br(4) are substantially larger. In fact, as noted in the structure solution, these bromine atoms are probably disordered off the mirror plane, with y coordinates slightly different from zero.

Magnetic Analysis

The plot of inverse molar susceptibility vs. absolute temperature is shown in Figure 4. The data exhibit two distinct linear regions: a high-temperature regime dominated by strongly antiferromagnetic (AFM) interactions ($\Theta = -132$ K) with a Curie constant slightly less than that for four independent copper ions; a low-temperature regime dominated by weakly antiferromagnetic interactions ($\Theta = -9$ K) and a Curie constant somewhat more than that of a single copper ion. Below 10 K, additional AFM coupling is apparent. The conclusion is that the high-temperature regime is dominated by strong AFM coupling within trimers, leading to a depopulation of the quartet state and the consequent occupation of the lowest doublet state. This gives a resultant value of $S = {}^1/_2$ per trimer. The low-temperature regime then corresponds to AFM coupling with each $(CuBr_2)_n$ chain. The further AFM coupling below 10 K is ascribed to interactions between trimers and/or between trimers and chains.

On the basis of this interpretation, the χ–T data (Figure 5) were fit to the model

$$\chi_M = \chi_t + \chi_c$$

where χ_t is the susceptibility expression for the stacks of trimers

$$\chi_t = \frac{C_{1/2}}{T-\Theta}\,\frac{2 + 2\exp(J/kt) + 20\exp(3J/kT)}{2 + 2\exp(J/kT) + 4\exp(3J/kT)}$$

with the assumption of equal g values for all three copper atoms, only nearest-neighbor interactions within the trimer, and Θ representing a mean-field approximation to the intertrimer interactions; χ_c is the susceptibility for a Heisenberg chain of spin ${}^1/_2$ ions interacting with a coupling constant J'.[28]

The dashed line in Figure 5 shows the least-squares fit of the model to the data over the temperature range 10–300 K, with $J/k = -100$ K, $J'/k = -21$ K, and $\Theta = 1.7$ K, and the Curie constants, $C_{1/2}$ and $C'_{1/2}$, fixed at 0.40. Attempts to vary the Curie constants simultaneously with the exchange parameters were unsuccessful. Since the mean-field term corresponds to a ferromagnetic coupling between trimers, the model clearly cannot account for the behavior of the data below 10 K. This indicates the presence of additional AFM interactions between the trimers and the chains. However, introduction of this interaction into the model yielded too many parameters, and the least-squares procedure failed to converge satisfactorily. Nevertheless, as discussed in the following section, the principal interactions are satisfactorily characterized and the failure of the models to fit the data below 10 K is not deemed a serious shortcoming.

Magneto–Structural Correlations

The theoretical framework for interpreting magneto–structural correlations in copper(II) salts was presented in a paper by Hay et al.,[29] where it was shown that the exchange coupling, $2J$, could be expressed in copper dimers as

$$2J = 2K_{ab} - 2(\epsilon_s - \epsilon_a)^2/(J_{aa} - J_{ab}) \qquad (1)$$

where K_{ab} and J_{aa}, J_{ab} are Coulomb and exchange integrals between the two metal atom centers and ϵ_s, ϵ_a are the one-electron orbital energies of the symmetric and antisymmetric combinations of the local magnetic orbitals. Girerd et al. have shown, in a slightly different formalism, that the same expression holds for $2J$ in cyclic chains as in dimers.[30] In eq 1 the Coulomb integral, K_{ab}, is inherently positive, as is the quantity $(J_{aa} - J_{ab})$. Thus, the exchange interaction is portioned into a ferromagnetic portion (K_{ab}) and an antiferromagnetic part. The latter depends on the square of the energy difference of the one-electron MOs derived from the local magnetic orbitals. This partitioning is conceptually very convenient. Hay et al. made the assumption that the Coulomb and exchange integrals are basically geometry independent, so that the gross features of the exchange coupling can be determined by the one-electron MO energies. This leads to the conclusion that J is positive (ferromagnetic) if the two magnetic orbitals are orthogonal and becomes progressively smaller as overlap increases. This has been exploited by Kahn and co-workers[31,32] in designing new heterobinuclear complexes. Kahn has also challenged the concept that the ferromagnetic term is geometry independent and proposed a method to estimate how K_{ab} varies.[33]

In the paper by Hay et al.[29] the effects of various distortions of $Cu_2Cl_6^{2-}$ dimers were examined within the extended Hückel framework. For the planar dimer, it was found that $\epsilon_s = \epsilon_a$ when the Cu–Cl–Cu bridging angle, ϕ, was 88°. This is not expected to be quantitative but points out that J is expected to be ferromagnetic when $\phi \sim 90°$, with the exchange becoming increasingly antiferromagnetic when ϕ deviates from this value. Experimentally, it has been found that J is ferromagnetic in copper(II) chloride salts with planar coordination when ϕ ranges between 85 and 90°[18] but antiferromagnetic for $\phi > 93°$.[16,17] Similar trends are expected to hold

(28) J. C. Bonner and M. E. Fisher, *Phys. Rev.* [*Sect.*] *A*, **135**, 640 (1964).
(29) P. J. Hay, J. C. Thibeault, and R. Hoffmann, *J. Am. Chem. Soc.*, **97**, 4884 (1975).
(30) J. Girerd, M. Charlot, and O. Kahn, *Mol. Phys.*, **34**, 1063 (1977).
(31) O. Kahn, *Inorg. Chim. Acta*, **62**, 3 (1982).
(32) O. Kahn, J. Galy, Y. Journaux, J. Jaud, and I. Morgenstern-Badarau, *J. Am. Chem. Soc.*, **104**, 2165 (1982).
(33) O. Kahn and M. F. Charlot, *Nouv. J. Chim.*, **4**, 567 (1980).

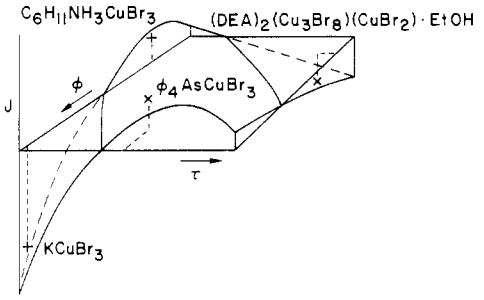

Figure 6. Schematic illustration of the $J(\phi,\tau)$ surface for symmetric bibridged copper(II) systems.

for the bromide salts in agreement with the results of this study.

The effect of changing the coordination geometry from square planar toward tetrahedral was also examined by Hay et al.[29] This distortion is characterized by the dihedral angle, τ, between the planes defined by the terminal CuX_2 fragment and the bridging CuX_2 fragment. For a ϕ value such that $J < 0$, it was found that, as ϕ increases from 0°, the interaction first becomes positive ($J > 0$), reaching a maximum, and then becomes negative again as ϕ approaches 90°. Experimentally, it is found that the planar dimer in $KCuCl_3$[22] is antiferromagnetic, while the twisted dimers in $Ph_4AsCuCl_3$[34] and Ph_4PCuCl_3[35] are ferromagnetic.

As indicated in the Introduction, structures are not known on many copper(II) bromide salts. Assuming isomorphism with the corresponding chlorides, we can begin to examine the magneto–structural correlations in the bromide series. For the planar dimers in $KCuBr_3$[36] and NH_4CuBr_3[16] ($\phi \sim 95°$; $\tau = 0°$), antiferromagnetic behavior is observed with $J/k \sim -100$ K. In $(C_6H_{11}NH_3)CuBr_3$ ($\phi \sim 86°$; $\tau = 0°$),[37] ferromagnetic behavior is found with $J/k \sim 60$ K. (It is noted that the copper geometry is square pyramidal and other distortions exist. However, $J > 0$ is also found in $CuBr_2 \cdot Me_2SO$,[38] where $\phi = 86°$.) Then in $Ph_4AsCuBr_3$[39] and Ph_4PCuBr_3[35] ($\phi \sim 93°$; $\tau \sim 48°$), ferromagnetic interactions are again found with $J/k \sim 30$ K. To this we add the results of this study where we have, for the trimer ($\phi \sim 94°$; $\tau = 0°$), $J/k = -100$ K and, for the chain ($\phi \sim 84°$; $\tau \sim 86°$), $J/k = -20$ K. These results can be interpreted qualitatively in terms of the $J(\phi,\tau)$ surface drawn schematically in Figure 6. For the lines with $\tau = 0°$ and with $\phi \sim 95°$, the qualitative features of the theoretical predictions of Hay et al.[29] are incorporated with the remainder of the curve deduced from eq 1. We see that a ferromagnetic ridge exists in the surface, with the antiferromagnetic trimer lying on one side of the ridge and the antiferromagnetic chain lying on the opposite side.

Finally, it is appropriate to comment on the difference between the approach we have taken in discussing magneto–structural relationships in systems with multiple structural parameters and those taken by several other authors. We are seeking to map out a hypersurface of the type, for example, $J(\phi,\tau)$. Contrariwise, it has been proposed, in hydroxy-bridged Cr(III) dimers[40] and in asymmetrical bridged copper(II) halide salts,[41] that J depends only on the ratio ϕ/R, where ϕ is the bridging angle and R is the Cr–O or the axial Cu–Cl distance. The latter can be valid in two situations if there is a strong correlation between the two parameters, ϕ and R: this may occur, for example, if (1) the bridging ligand–ligand repulsions determining the bridging geometry or (2) the paths of constant ϕ/R are essentially parallel to contours of constant J. It is clear, in any case, that a ratio of structure parameters such as ϕ/R only samples a portion of the total surface defining the exchange energy.

Acknowledgment. This work was supported by NSF Grant No. CHE-77-08610.

Registry No. $(DEA)_2Cu_4Br_{10} \cdot EtOH$, 83632-64-8.

Supplementary Material Available: Listings of positional and thermal parameters and observed and calculated structure factors (7 pages). Ordering information is given on any current masthead page.

(34) C. Chow and R. D. Willett, *J. Chem. Phys.*, **59**, 5903 (1973).
(35) W. E. Estes, J. R. Wasson, J. W. Hall, and W. E. Hatfield, *Inorg. Chem.*, **17**, 365 (1978).
(36) M. Inoue, M. Kishita, and M. Kubo, *Inorg. Chem.*, **6**, 900 (1967).
(37) R. D. Willett, C. P. Landee, R. M. Gaura, D. D. Swank, H. A. Groenendijk, and A. J. van Duyneveldt, *J. Magn. Magn. Mater.*, **15-18**, 1055 (1980).
(38) D. D. Swank, private communication.
(39) C. Chow, R. D. Willett, and B. C. Gerstein, *Inorg. Chem.*, **14**, 205 (1975).
(40) R. P. Scaringe, W. E. Hatfield, D. J. Hodgson, *Inorg. Chem.*, **16**, 1600 (1977).
(41) W. E. Hatfield, R. R. Weller, and J. W. Hall, *Inorg. Chem.*, **19**, 3824 (1980).

Contribution from Ames Laboratory and the Department of Chemistry, Iowa State University, Ames, Iowa 50011

Kinetics of the Reduction of Pyridinium Ions by 2-Hydroxy-2-propyl Radicals in Aqueous Solution

MAKOTO SHIMURA and JAMES H. ESPENSON*

Received July 9, 1982

Kinetic measurements were made for the reductions of the pyridinium ions derived from pyridine, 4-methylpyridine, 3-hydroxypyridine, nicotinamide, and isonicotinamide as well as 1-methylpyridinium and 1,4-dimethylpyridinium ions by 2-hydroxy-2-propyl radicals, which were generated by the homolytic cleavage of the chromium–carbon bond in $(H_2O)_5CrC(CH_3)_2OH^{2+}$. The rate constants ($dm^3\ mol^{-1}\ s^{-1}$) at 25.0 °C and an ionic strength of 1.0 M ($LiClO_4$) are as follows: pyridinium ion, 9.6×10^5; 1-methylpyridinium ion, 3.7×10^5; 4-methylpyridinium ion, 7.3×10^4; 1,4-dimethylpyridinium ion, $\leq 1 \times 10^4$; 3-hydroxypyridinium ion, 1.4×10^8; 3-(aminocarbonyl)pyridinium ion, 7.9×10^8; 4-(aminocarbonyl)pyridinium ion, 1.2×10^9. The rate constants are reasonably well correlated by the Hammett ρ–σ equation with $\rho = +8.5$. The first two compounds show a second kinetic term corresponding to the rate law $k'[Cr^{2+}][pyH^+][\cdot C(CH_3)_2OH][H^+]^{-1}$, consistent with reduction of a Cr(II)–pyridine complex by the free radical.

Introduction

Homolytic cleavage of the chromium–carbon bond in $(H_2O)_5CrC(CH_3)_2OH^{2+}$ is a ready source of 2-hydroxy-2-propyl radicals and, as recently demonstrated,[1] can be used for kinetic studies of the reactions of 2-hydroxy-2-propyl radicals in acidic solutions. Reductions of cobalt(III)–amine

(1) Espenson, J. H.; Shimura, M.; Bakač, A. *Inorg. Chem.* **1982**, *21*, 2537.

0020-1669/83/1322-0334$01.50/0